CTFF3 TECHNICAL NOTE

INFN - LNF, Accelerator Division

LINEAR OPTICAL MODEL OF CTF3 WIGGLERS

C. Biscari

1. Introduction

In CTF3 two wigglers are used for trajectory length tuning, one in the Delay Loop, the other one in the Combiner Ring [1].

The characteristics of the wigglers are given in [1-2], while the magnetic measurements corresponding to the integrated value of the field performed on one of the two magnets are described in [3]. The field map inside the wiggler has been simulated [4] with the OPERA code, and not measured. Figure 1 shows the wiggler view from the side and a sketch of the wiggler layout.

In order to describe in optical codes the effect of the wiggler on beam dynamics, an optical model is needed.

The field components in any point in a region near the axis are described analytically, and used for tracking purposes. The Jacobian around the trajectory is then used to define the optical model parameters.
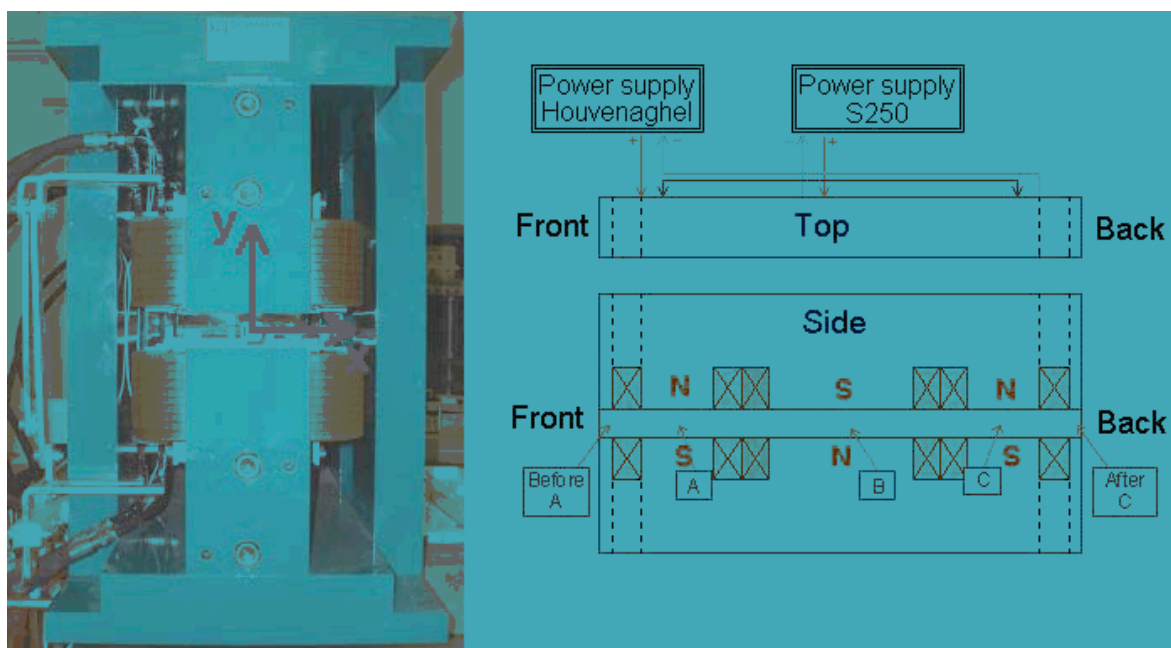

Figure 1 – CTF3 Wiggler view.

2. Multipolar analysis and analytical expression for magnetic fields.

Let's recall some well known properties of magnetic field for completeness. The general scalar magnetic multipolar potential of order m in cylindrical coordinates can be written as (see for example [5]):

$$P_m(r,\theta,z) = \frac{r^m \sin m\theta}{m!} G_m(r,z) \qquad \qquad 1)$$

where the condition of satisfying the Laplace equation is equivalent to:

$$\frac{\partial^2 G_m}{\partial r} + \frac{2m+1}{r}\frac{\partial G_m}{\partial r} + \frac{\partial^2 G_m}{\partial z^2} = 0 \qquad \qquad 2)$$

Writing the solution of 2) as:

$$G_m(r,z) = \sum_{k=0}^{\infty} G_{m2k}(z) r^{2k} \qquad \qquad 3)$$

one can demonstrate that:

$$G_{m2k}(z) = (-1)^k \frac{m!}{4^k (m+k)k!} \frac{\partial^{2k} G_{m0}}{\partial z^{2k}} \qquad \qquad 4)$$

If there is no dependence on z, the potential contains only the first term of the sum 4) for each multipole: for example a pure dipole is described in cylindrical coordinates by:

$$P_1(r,\theta) = r \sin\theta\, G_{10} \qquad \qquad 5)$$

while if there is dependence on z, as in the wiggler case, the dipole potential becomes:

$$P_1(r,\theta,z) = r \sin\theta \left[G_{10}(z) + G_{12}(z)r^2 + G_{14}(z)r^4 + \ldots \right] \qquad \qquad 6)$$

where by writing $G_{m2p+1}(z)$ we mean the derivative with respect to z of $G_{m2p}(z)$:

$$G_{m\,2p+1}(z) = \frac{dG_{m\,2p}(z)}{dz} \qquad \qquad 7)$$

The vertical field component along the wiggler axis $B_y(0,0,z)$ coincides with $G_{10}(z)$. The term G_{12} is called the pseudo sextupole, since the magnetic field component deriving from it has a quadratic behaviour in the coordinates.

A normal sextupolar magnetic potential with dependence on z is given by $P_3(r, \theta, z)$:

$$P_3\left(r,\theta,z\right)= \frac{r^3 \sin 3\theta}{3!}\left[G_{30}\left(z\right)+ G_{32}\left(z\right)r^2 +...\right] \qquad 8)$$

The wiggler potential can be fitted with a dipole plus the higher order components, as sextupole, decapole, etc. The magnetic field is directly derived from Eqs. 6 and 8 as the gradient of the scalar magnetic potential.

Keeping only terms up to the second order, we maintain the dipole and the sextupole. The magnetic field components in cylindrical coordinates are then:

$$B_r(r,\theta,z) = \sin\theta \left[G_{10}(z) + 3\,G_{12}(z)\,r^2\right] + \frac{1}{2}\sin 3\theta\,G_{30}(z)\,r^2$$

$$B_\theta(r,\theta,z) = \cos\theta \left[G_{10}(z) + G_{12}(z)\,r^2\right] + \frac{1}{2}\cos 3\theta\,G_{30}(z)\,r^2 \qquad 9)$$

$$B_z(r,\theta,z) = \sin\theta\,G_{11}(z)\,r$$

From these expressions, the vertical field component on the wiggler axis is simply:

$$B_y(0,0,z) = G_{10}(z) \qquad 10)$$

Both magnetic measurements and magnet simulation codes provide the value of the vertical magnetic component B_y. Knowing the function G_{10}, it is possible to derive all magnetic components coming from the dipolar field in every point of the space inside the magnet. For obtaining the sextupolar term the vertical field must be known also at different values of r.

Let's recall here that the function $G_{m0}(z)$ can be expressed analytically if we consider the magnetic potential as produced by a cylindrical surface with a m-pole current distribution [5]. Being R the radius of the cylinder, $2Z$ its total length, and I_c the current, we define:

$$t_1 = Z - z$$
$$t_2 = -Z - z$$
$$A(t) = \sqrt{R^2 + t^2} \qquad 11)$$
$$f_h(t) = \left(\frac{t}{A}\right)^h \quad (h = 0,1,...\infty)$$

$G_{m0}(z)$ can be written as:

$$G_{m0}(z) = G_{m0}(t_1) - G_{m0}(t_2) \qquad 12)$$

where:

$$G_{m0}(t) = \mu_o I_c \frac{(2m-1)}{R^m 4^m (m-1)!} \sum_{k=0}^{m} (-1)^k \frac{m+k+1}{2k+1} \binom{m}{k} f_{2k+1}(t) \qquad 13)$$

The three parameters R, Z, and I_c can be used to fit the measured or simulated magnetic field on axis with the analytical expression 13).

In particular the functions $G_{mn}(t)$ appearing in Eq. 9) can be written in terms of the functions $f_h(t)$:

$$G_{10}(t) = \frac{\mu_o I_c}{4R} \left[2 f_1(t) - f_3(t) \right]$$

$$G_{11}(t) = \frac{\mu_o I_c}{4} \frac{R}{A^3} \left[2 - 3 f_2(t) \right]$$

$$G_{12}(t) = -\frac{1}{8} \frac{\mu_o I_c}{4R^3} \left[2(-3 f_1(t) + 6 f_3(t) - 3 f_5(t)) - (6 f_1(t) - 27 f_3(t) + 36 f_5(t) - 15 f_7(t)) \right] \qquad 14)$$

$$G_{30}(t) = \frac{15}{16} \frac{\mu_o I_c}{R^3} \left[4 f_1(t) - 5 f_3(t) + \frac{18}{5} f_5(t) - f_7(t) \right]$$

Writing the cartesian field components :

$$B_x(x,y,z) = 2xy G_{12}(z) + r^2 \cos 4\theta \, G_{30}(z)/2$$

$$B_y(x,y,z) = G_{10}(z) + (3y^2 + x^2) G_{12}(z) + r^2 \sin 4\theta \, G_{30}(z)/2 \qquad 15)$$

$$B_x(x,y,z) = y G_{11}(z)$$

A Matlab code generating these expressions has been written, and can be easily extended to different kinds of wigglers.

3. CTF3 Wiggler.

The CTF3 wiggler is a three pole wiggler, used to tune the trajectory length in a range of ± 4 mm [1]. The magnetic field characteristics have been calculated with the code OPERA, in 3D. Figures 2-3 show the simulated vertical field component along z for half the wiggler, in the median plane and in the vertical plane respectively. Figure 4 shows the integral of the vertical field component along z for different values of the transverse coordinates.

To be noticed in Fig. 3 the behaviour of B_y as the vertical coordinate increases, and the region approaches the magnet iron. This behaviour cannot be reproduced with the analytical function which reproduces a cylindrical symmetry, but in any case it corresponds to high values of y,

not interesting for the tracking purposes. It is more important to reproduce the sextupole behaviour of the field in the horizontal plane, where the trajectory excursion is large.

In principle it is possible also to use higher order multipoles to better fit the field components, but in this first approximation we deal only up to the 2nd order terms.
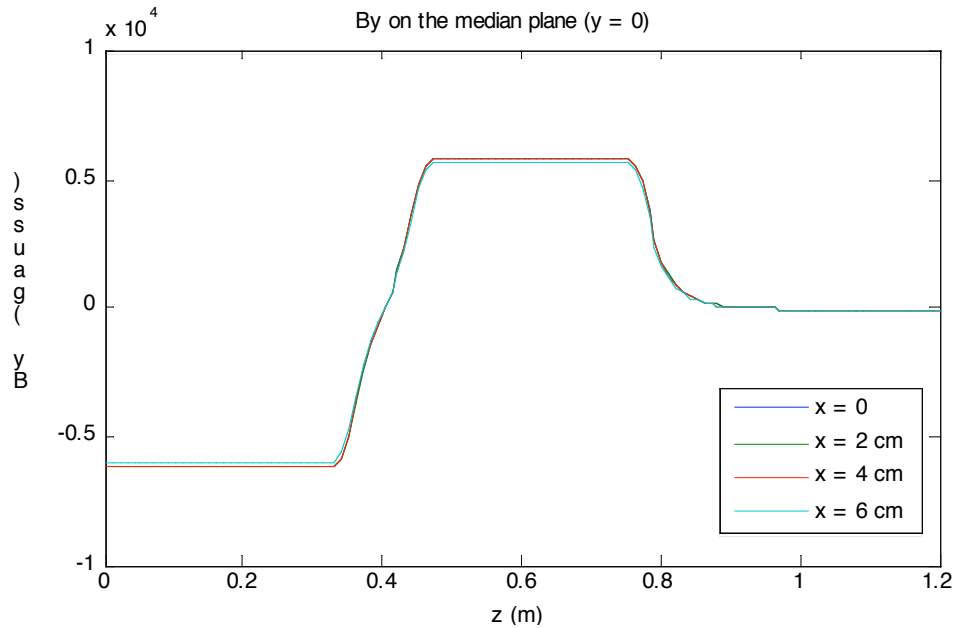
Figure 2 – By(z) along half a wiggler in the median plane – OPERA simulations.
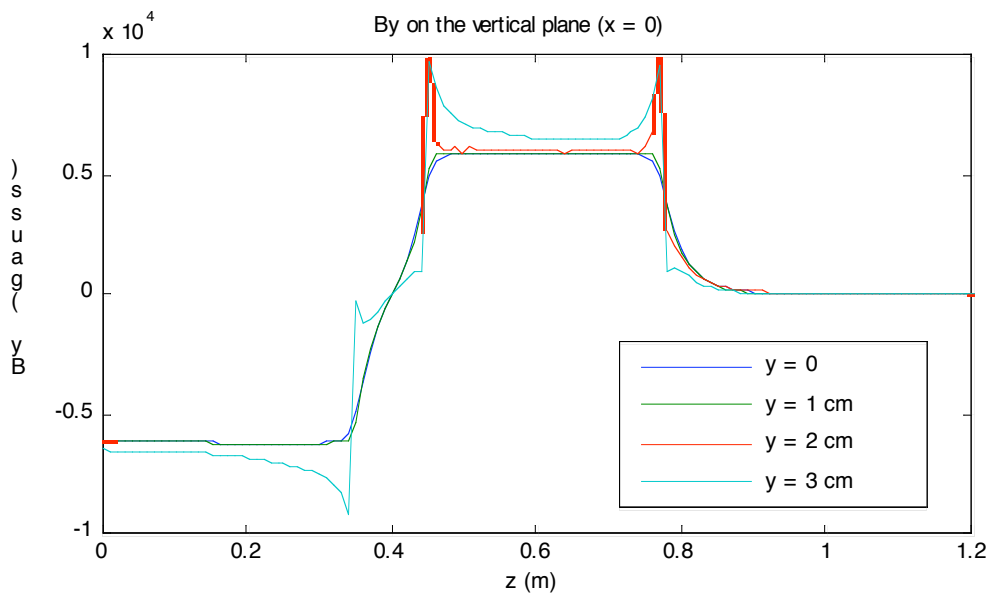
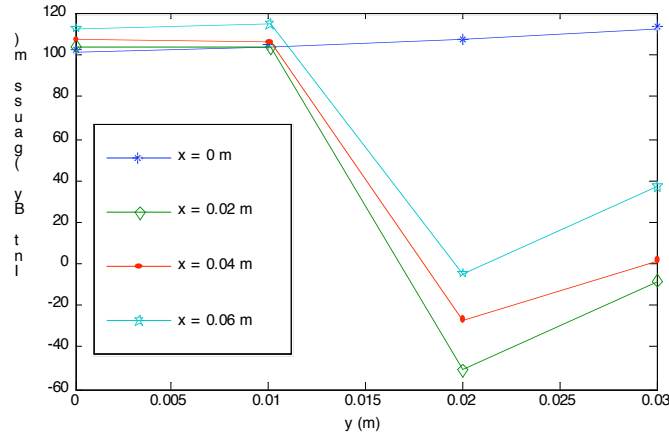Figure 3 – $B_y(z)$ along half a wiggler in the vertical plane – OPERA simulation.

Figure 4 – Integrated $B_y(z)$ along half a wiggler – OPERA simulations.

Fitting the function represented in Fig. 2 with the analytical expression of Eq. 13 can be done with a very good approximation, using a superposition of several current distributions, each one of them defined by its three fitting parameters.

In order to reduce the CPU time for all the following calculations, we have chosen the minimum number of current distributions, relaxing the condition of exactly fitting the $G_{10}(z)$ function, and maintaining in any case a good representation of the transverse behaviour of the field along the wiggler, specially in the central pole, where the trajectory has its maximum deviation from the axis, and the field has the maximum absolute value.

Therefore we have chosen only one dipolar and one sextupolar current distribution for each one of the poles. The fitting parameters of such distributions are shown in Table I. The value of I_c is normalized to the value of the parameter of the central pole (I_{cent} = 2e5 A corresponds roughly to a field at the wiggler center of 0.1T) and of course no effect of saturation is considered, since the maximum available field is 0.6 T. Z_o represents the longitudinal coordinate of the current distribution center.

Table I – Fitting parameters for current distributions of CTF3 wiggler.

	Central Pole Dipole	Central Pole Sextupole	End Pole Dipole	End Pole Sextupole
Z (m)	0.365	0.365	0.18	0.18
R (m)	0.042	0.042	0.046	0.046
I_c / I_{cent}	1	-0.002	-1.109	0.0036
Z_o (m)	0	0	0.61	0.61

Figure 5 shows the vertical field along z in the analytical computation (red full line) compared to the OPERA simulation (blue dashed line), along half wiggler and Figures 6-7 show the first and second derivative along z. The analytical expression reproduces well the integral of each component, even if it not exactly the behaviour. For tracking purpose this is a satisfying representation of the field. A better representation, as already said before, would need a larger number of different current distributions for each pole, instead of only one.

The value of the sextupolar current distribution has been adjusted in order to fit the horizontal behaviour of the integral along *z* of the vertical field component, as shown in Fig. 8. In this figure the value of the integral of the magnetic field vertical component along the wiggler axis is not exactly zero, since it corresponds to the OPERA simulations, which gave such a residual integrated value. The zero integral can be obtained by changing the relative currents of the central and end poles, as shown in the table I. In practice the relative values between the poles must be adjusted to give zero integral on the beam trajectory instead that on the axis, as will be shown in the following.
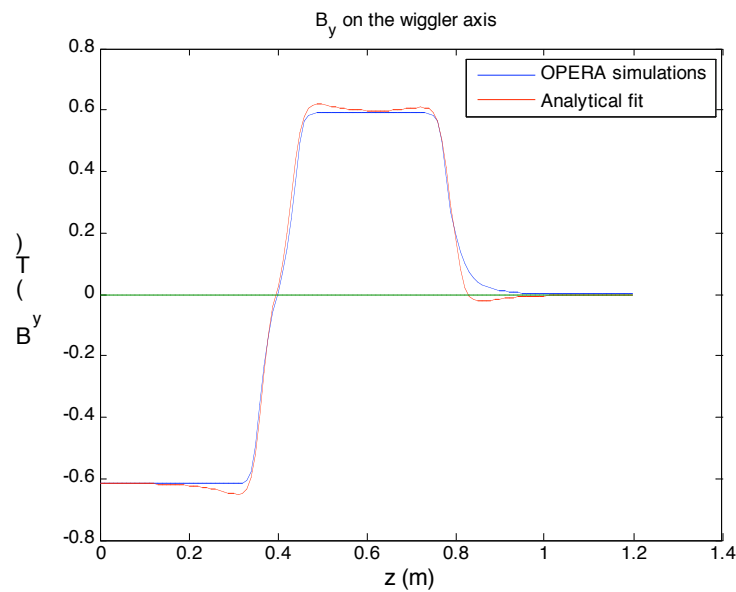
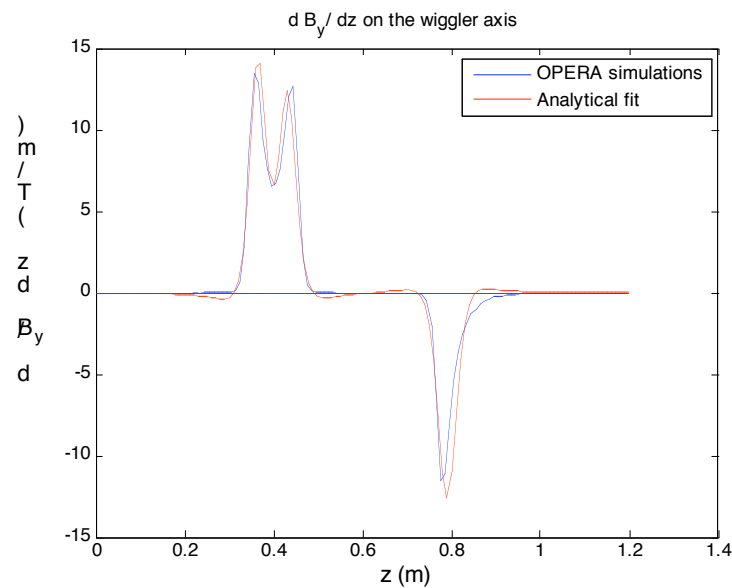Figure 5 – Vertical field component on the wiggler axis for half a wiggler.

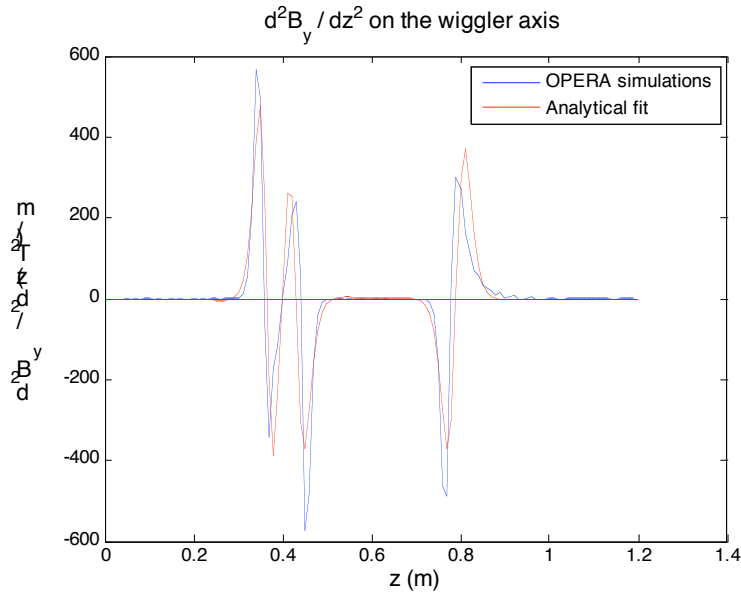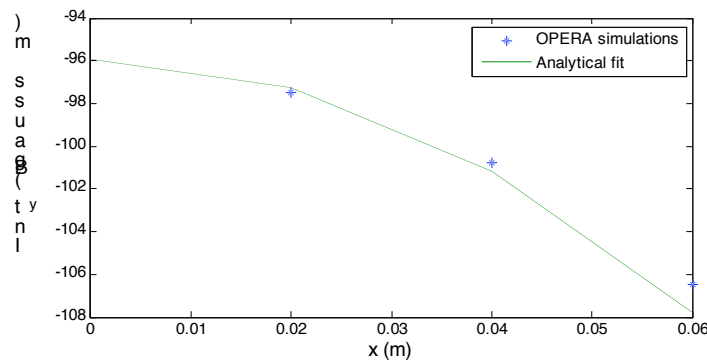Figure 6 – First derivative of the vertical field component.

Figure 7 – Second derivative of the vertical field component.

Figure 8 – Integral of vertical field component along z as a function of the horizontal coordinate.

4. Beam trajectory and Wiggler transfer matrix.

A dedicated Matlab code has been written to compute the beam trajectory inside the wiggler and the first order transport matrix around the trajectory. The magnetic field is defined by the expressions 9) in any point around the wiggler axis in a region including the wiggler and two adjacent drifts, to take care of the fringing fields.

The nominal trajectory in the two wigglers of the CTF3 complex corresponds to an increase of the path with respect to the wiggler length of $\Delta l = 4$ mm. Tuning the wiggler field, Δl can be varied from zero (wiggler off) to about 1 cm. Figure 9 shows six different trajectories, corresponding to $\Delta l = 0$, 1.2, 2.7, 4.8, 7.5, 10.9 mm. Both wigglers are aligned with their axis shifted by 2.5 cm toward the centre of the rings [6], so that the nominal trajectory wigglers around the magnet axis. This means that the beam enters the wiggler in any case at a position of -2.5 cm from the axis, as shown in Fig. 9, where the zero position of the coordinate x corresponds to the geometric wiggler axis.
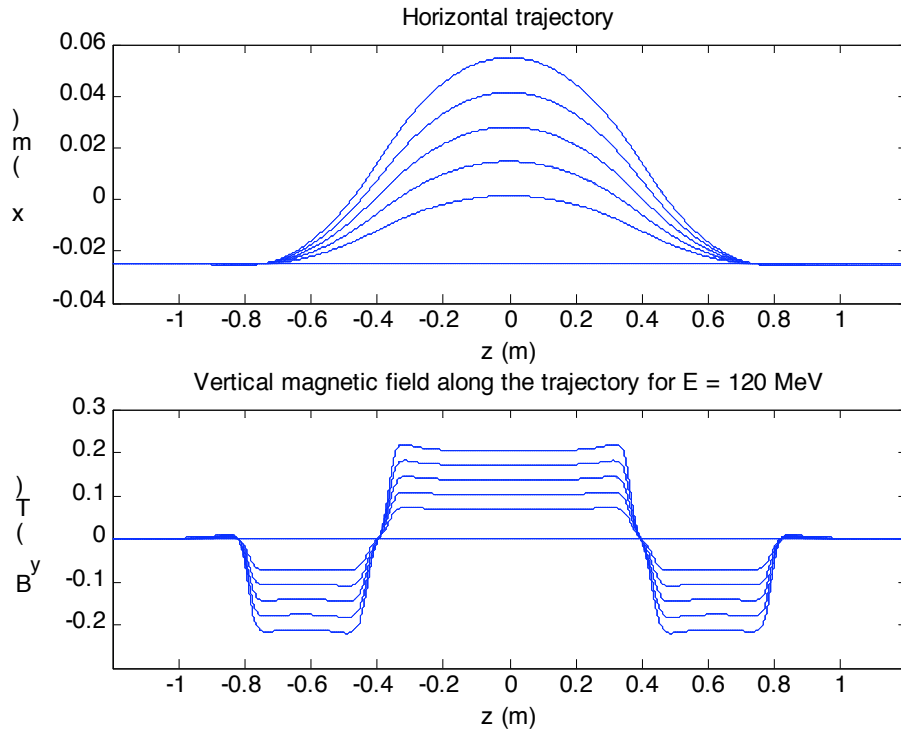
Figure 9 – Beam trajectory along the wiggler, corresponding to different values of Δl, and B_y along the trajectory for $E = 120$MeV.

Figure 10 shows the value of the trajectory distance from the wiggler axis as a function of the elongation Δl, and the corresponding field at the wiggler center, for an energy of 120 MeV, which is the usual beam energy in 2007.
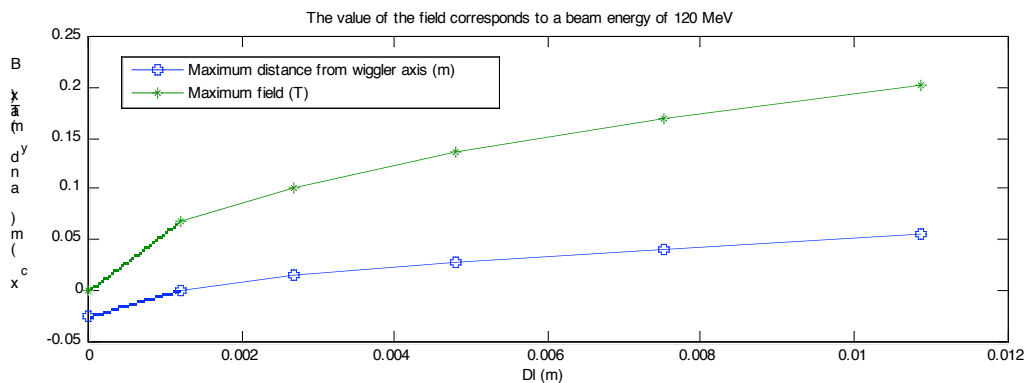

Figure 10 – Field at wiggler center (E = 120MeV) and horizontal distance of the beam trajectory from the wiggler axis.

The wiggler configuration with zero field integral along the axis does not correspond to zero field integral along the trajectory, due to the field dependence on the horizontal coordinate. Compensating the field along the trajectory is done by adjusting the central pole field with respect to the end poles, as shown in figure 11, which shows the factor I_{cf} for which I_{cent} is multiplied as a function of Δl to obtain zero integral along the trajectory. This correction factor is in any case smaller that 1%, and it can be neglected in the usual ring operation.
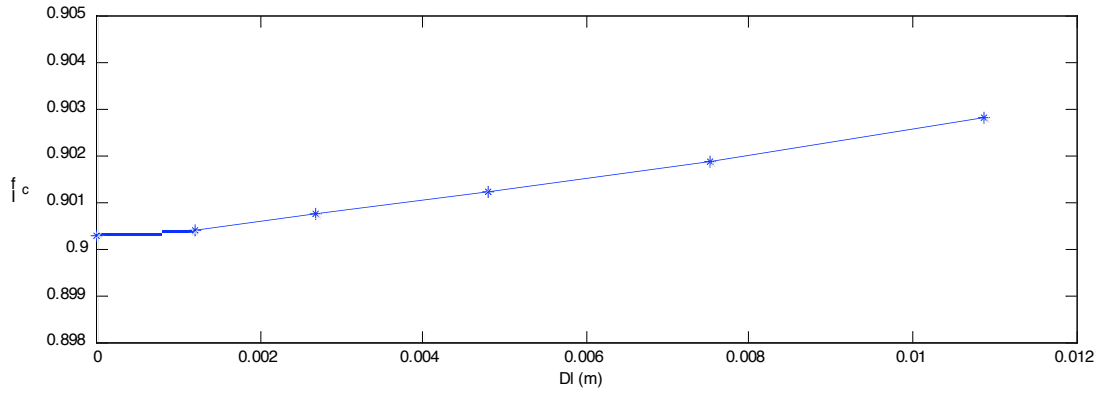
Figure 11 – Compensation factor for central pole (I_{cf} = 0.9015 corresponds to zero integral field on the wiggler axis.

The Jacobian around the trajectory extended ±1.2 m from the wiggler center has been computed for different values of Δl with the home written MATLAB code. Let the vector **X** represent the particle coordinates:

$$\mathbf{X} = (x, x', y, y', \delta l, \delta p / p) = (x_i), \quad i = 1, ...6 \tag{15}$$

and $\mathbf{X}^{In}$, $\mathbf{X}^{Fn}$ the initial and final coordinates of the trajectory around which the transport matrix is to be calculated.

By tracking the $j = 1,...6$ particles with initial coordinates $\mathbf{X}^{Ij} = \mathbf{X}^{In}$ except for the j-th coordinate, which is $x_j^{Ij} = x_j^{In} + \partial x_j$, the corresponding final coordinates are $\mathbf{X}^{Fj}$.

In first order approximation, the coordinates of a particle after the passage in the wiggler around the trajectory defined by $\mathbf{X}^{In}$ and $\mathbf{X}^{Fn}$ can be written as:

$$\mathbf{X}^f = \mathbf{J}\,\mathbf{X}^i \tag{16}$$

where the Jacobian **J** terms are defined as:

$$J_{ij} = \frac{x_i^{Fj} - x_i^{Fn}}{\partial x_j} \tag{17}$$

Two terms per plane of the Jacobian are shown in Figure 12. Since the system is symmetric around the wiggler center, the terms $J_{i+1\,i+1} = J_{ii}$ ($i = 1,3$) and the 4th term is given by det (**J**) =1.
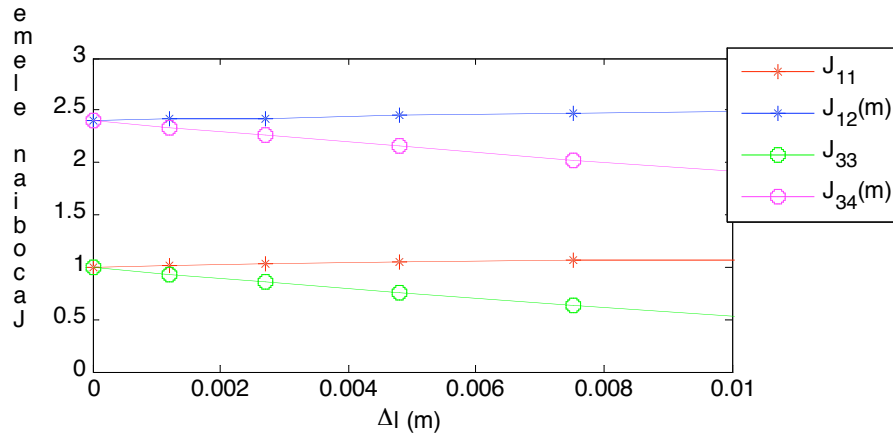
Figure 12 – Jacobian terms around the trajectory as a function of the trajectory elongation.

5.   Linear optical model for the Wiggler.

The optical model describing the wiggler in the MAD code is a sequence of rectangular bendings. Each pole is defined by three bends, an inner one with a stronger field, and two lateral with lower fields, in order to describe the fringing field. Such model does not take into account the effect of the dropout of the field on the transverse direction. The values of the 1st order transport matrix for the 2.4m long line centered around the wiggler midpoint are shown in Fig. 13, compared with those obtained by tracking in Fig. 12. It can be noticed that the terms corresponding to the horizontal plane behave, as expected, as the terms of a drift matrix ($R_{11} = 1.$, R_{12} = trajectory length).

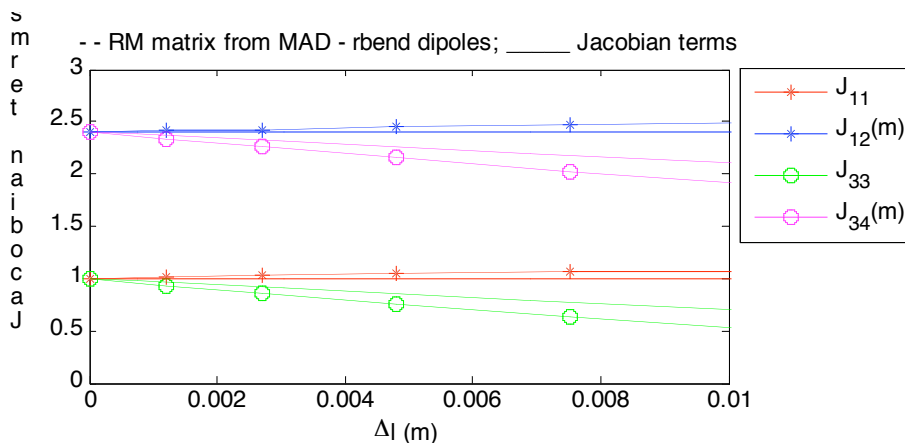Figure 13 – MAD 1st order transport matrix elements with rectangular bends modelling and no thin quadrupolar lenses (dashed lines) compared to the Jacobian terms (full lines).

In order to take into account the multipolar analysis, a series of quadrupolar thin lenses has been inserted in the model (see Fig. 14), and fitted their values to match the Jacobian terms as

obtained by tracking. Figure 15 shows the strength of the quadrupolar lenses as a function of the elongation Δl.

The optical model obtained with the new matrix fits well the measured response matrix [7].
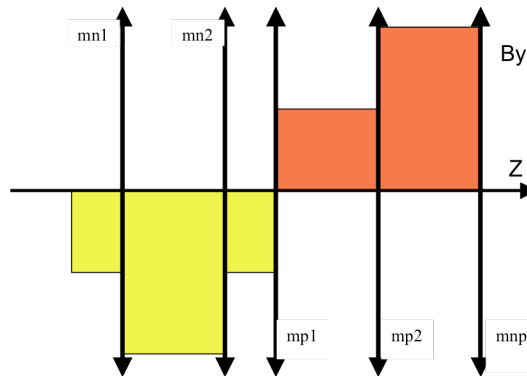

Figure 14 – Sketch of the vertical magnetic field used in the MADX optical model for half a wiggler. The arrows indicate the quadrupolar thin lenses.
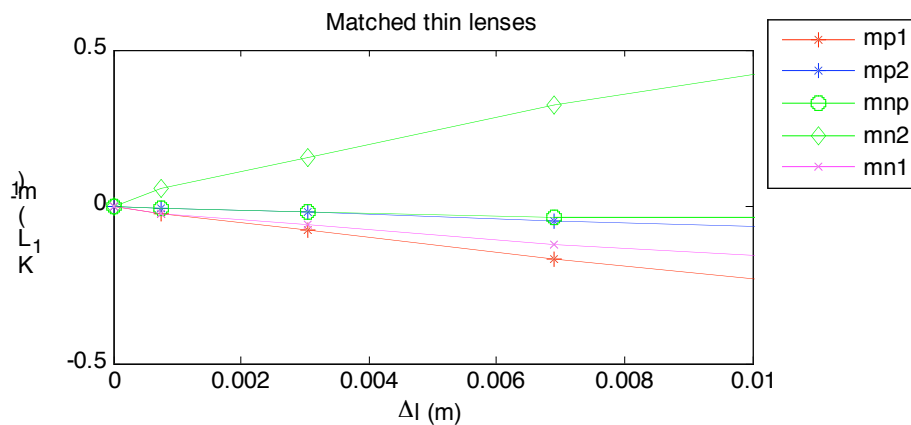

Figure 15 – MAD matching values for the quadrupolar lenses accounting for the transverse behaviour of the wiggler field as a function of the trajectory elongation.

5.   Conclusions

An analytical description of the CTF3 wiggler field fitting the magnetic field simulations has been done. The linear optical model of the wiggler to be used in tracking codes and in the optical description of the CTF3 Delay Loop and Combiner Ring has been deduced.

The derivation of the non linear model is in progress, together with a more accurate description which includes also an octupolar term in the description, better fitting the transverse behaviour of the wiggler field.

References

[1]   C. Biscari, "Combiner ring lattice", CTFF3-002, 2001.

[2]   C. Biscari, "New Design for the Delay Loop in CTF3", CTFF3-006, 2002.

[3]   P. Leclère, M. Silva, R. Woloszyn, "Magnetic measurements of the CTF3 Wiggler", AT-MTM-IN-2006-030.

[4]   C. Sanelli, private communication.

[5]   M. Bassetti, C. Biscari, "Analytical Formulae for Magnetic Multipoles", Particle Accelerator, 1996, Vol. 52, pp. 221-250.

[6]   L. Rinolfi, private communication.

[7]   P.K. Skowronski, CTF3 Collaboration Meeting, CERN, January 2008.